ELSEVIER

Journal of Contaminant Hydrology 37 (1999) 139–157

JOURNAL OF
Contaminant
Hydrology

Influence of diameter on particle transport in a fractured shale saprolite

D.H. Cumbie [a,1], L.D. McKay [b,*]

[a] *Kentucky Geological Survey, University of Kentucky, Lexington, KY 40506-0107, USA*
[b] *Department of Geological Science, University of Tennessee, Knoxville, TN 37996, USA*

Received 19 January 1998; revised 28 October 1998; accepted 28 October 1998

Abstract

Experiments in an undisturbed, saturated column of weathered and fractured shale saprolite using fluorescent carboxylate-coated latex microspheres as tracers indicate that particle diameter plays a major role in controlling transport. In this study the optimum microsphere diameter for transport was approximately 0.5 μm. Microspheres larger than the optimum size were present in the effluent at lower relative concentrations, apparently because of greater retention due to gravitational settling and/or physical straining. The smaller than optimum microspheres also experienced greater retention, apparently related to their higher rates of diffusion. Faster diffusion can lead to more frequent collisions with, and attachment to, fracture walls and may also lead to movement of particles into zones of relatively immobile pore water in the fractures or in the fine pore structure of the clay-rich matrix between fractures. Dismantling of the soil column and mapping of the distribution of retained microspheres indicated that there was substantial size-segregation of the microspheres between different fractures or in 'channels' within a fracture. Examination of small core samples showed that the smallest microspheres (0.05–0.1 μm) were present in the fine pores of the matrix at distances of up to 3–4 mm from the nearest fracture, which supports the hypothesis that small particles can be retained by diffusion into the matrix. Calculations of settling velocity and diffusion rate using simple 1D approaches suggest that these processes could both cause significant retention of the larger and smaller particles, respectively, even for the fast advective transport rates (up to 32 m/day) observed during the experiments.

Keywords: Particles; Colloids; Contaminant transport; Ground water; Fractures; Saprolite

* Corresponding author. Fax: + 1-423-974-2368; e-mail: lmckay@utk.edu
[1] E-mail: dcumbie@kgs.mm.uky.edu.

0169-7722/99/$ - see front matter © 1999 Elsevier Science B.V. All rights reserved.
PII: S0169-7722(98)00156-9

1. Introduction

Field and laboratory tracer experiments in fractured clay tills (McKay et al., 1993a,b; Hinsby et al., 1996) and clay-rich shale saprolite (McKay et al., 1995; Harton, 1996), under hydraulic gradients that are typical of field conditions, show that colloid-sized particles can be transported by flowing groundwater at relatively rapid rates (meters to tens of meters per day) and over significant distances (4 to >35 m). These rates are much higher than transport rates typically observed for colloidal tracers under natural gradient conditions in sandy aquifer materials (Harvey et al., 1989; Bales et al., 1995), likely because flow in clay-rich soils is usually concentrated in the fractures, whereas flow is more widely-distributed in sands. The above studies also indicate that colloid retention rates in the fractured clay-rich soils are higher than rates typically observed in aquifer sands. This suggests that although colloidal contaminants, such as pathogenic microorganisms or radionuclides attached to mobile particles, may travel rapidly in fractured clay-rich materials, the spatial extent of contamination may be relatively limited. Contaminant migration in these widespread soils may still be significant because in many areas these soils overlie aquifers or are adjacent to streams. Hence, there is a need to develop a better understanding of the physical and chemical processes influencing colloid transport in these materials.

Most previous theoretical and experimental investigations of particle transport in groundwater address transport in granular media, typically aquifer sands or glass beads (including Yao et al., 1971; Wang et al., 1981; McDowell-Boyer et al., 1986; Elimelech and O'Melia, 1990; Fontes et al., 1991; Bales et al., 1993; Harvey et al., 1993; Kinoshita et al., 1993; McCaulou et al., 1995). Investigations in fractured materials often focus on particle transport in volcanic or crystalline rocks (including Champ and Schroeter, 1988; Bales et al., 1989; Reimus, 1995; Vilks and Bachinski, 1996; Vilks et al., 1997), or in artificial fractures (Toran and Palumbo, 1992; Meinders et al., 1992). Relatively few investigations address particle transport in fractured or macropore-dominated clay-rich materials (Smith et al., 1985; McKay et al., 1993b; McKay et al., 1995; Kretzschmar et al., 1995; Hinsby et al., 1996; Harton, 1996) and it is uncertain whether findings obtained from studies of other materials are applicable to fractured clays.

Two experimental investigations of colloid transport in fractured or macropore-dominated clay-rich materials (Smith et al., 1985; Harton, 1996) showed that colloid retention is strongly influenced by flow rate, which is consistent with previous experimental studies of colloid transport in granular materials (Wollum and Cassel, 1978; Wang et al., 1981; Tan et al., 1994). Size of the mobile particles is also expected to be an important factor influencing colloid transport in fractured clay-rich materials. Reimus (1995) presented conceptual models for size-related colloid retention processes in fractures, based on an analogy to colloid filtration theory (Yao et al., 1971), which was initially developed for granular materials. The models predict the existence of an optimum particle size for transport, with greater retention of larger than optimum particles due to gravitational settling or due to straining in small aperture regions of the fractures. The smaller than optimum particles experience greater losses due to more rapid diffusion within the fracture, and hence more frequent collisions with, and attachment to, the walls of the fracture. There is also the possibility of greater diffusion

of small particles into relatively immobile water in small aperture regions within the fractures, or into the fine pore structure of the clay-rich matrix between fractures.

The overall objective of this study is to determine the influence of particle size on transport in a fractured clay-rich saprolite. Specific objectives include determining whether there is an optimum size range for transport of particles in this material, investigating possible retention mechanisms, and determining the influence of fracture characteristics on colloid distribution.

2. Site hydrogeology

The column of undisturbed soil used in the experimental investigation was collected from the proposed Solid Waste Storage Area 7 (SWSA-7) on the Oak Ridge Reservation in eastern Tennessee. The material is a highly weathered and fractured shale saprolite formed in situ by extensive leaching of the parent material, which is the Dismal Gap formation of the middle to upper Cambrian Conasauga Group (Hatcher et al., 1992). The saprolite retains the bedding, fractures and structure of the interbedded shales and limestones of the Dismal Gap formation, which was intensely deformed by regional tectonic activity. Where exposed, the formation has weathered to a saprolite varying in thickness from < 1 to 10 m (Solomon et al., 1992). Carbonates in this upper zone have been leached, leaving primarily illitic clays (Jardine et al., 1993). Many of the bedding planes and fracture surfaces are stained with coatings of Fe and Mn oxides, and can contain translocated clay minerals (Wilson et al., 1992). Hydraulic conductivity values in the upper 2 m of the saprolite range from 4×10^{-6} to 1×10^{-4} m/s (Wilson et al., 1992; Harton, 1996; Cropper, 1998).

3. Materials and methods

3.1. Column collection and set-up

The method used for collecting the soil column for this study is described in detail in Cumbie (1997) and generally followed the methods developed by previous researchers at the site (Jardine et al., 1988, 1993; Harton, 1996). A cylindrical sample of undisturbed shale saprolite was collected from a hand dug excavation at a depth of 1.2 m and was encased in a PVC pipe, with paraffin wax filling the annular space between the soil and the casing (Fig. 1). The column was set up in an inverted position with upward flow entering the original 'top' of the sample. The sample was saturated with a 0.005 M $CaCl_2$ solution which was also used as the influent solution for hydraulic conductivity measurements carried out before and after each tracer experiment.

3.2. Tracers and analytical methods

The colloidal tracers consisted of monodisperse fluorescent latex microspheres (Polysciences, 1995) with carboxylate surface coatings. Six different sizes of microspheres,

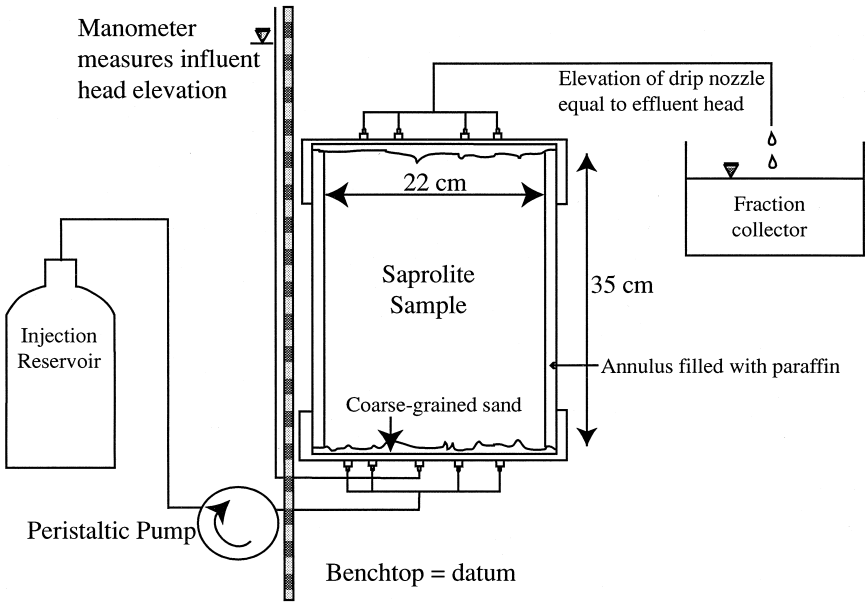

Fig. 1. Laboratory column set-up.

ranging in diameter from 0.05 to 4.25 μm, and two different fluorescent colors, yellow-green (YG) and blue (BB), were used in the experiments (Table 1).

Microsphere concentrations in the water samples were determined by filtration and epi-fluorescent microscopy. Water samples were vacuum-filtered through 25 mm polymembrane filters previously dyed black in a solution of 1 l 2.5% acetic acid and 2 g Irgalan Black dye. The filters were then mounted on glass slides and microspheres were

Table 1
Experimental results

	Tracer	Color	Average injection concentration	Maximum C/C_0 in effluent[b]	Recovery in effluent (%)[c]
Experiment number 1[a]	0.05 μm	YG	$2.9–3.0\times10^8$/ml	0.0012	0.14
	0.1 μm	BB	$3.6–4.5\times10^8$/ml	0.003	0.28
	0.5 μm	YG	$8.2–8.4\times10^6$/ml	0.17	1.4
	1.0 μm	BB	$7.0–7.5\times10^6$/ml	0.07	1.0
	Bromide	–	940 mg/l	0.81	93
Experiment number 2[a]	0.5 μm	YG	$7.0–7.1\times10^7$/ml	0.036	1.2
	1.7 μm	BB	$6.6–7.2\times10^5$/ml	0.0057	0.83
	4.25 μm	YG	$4.4–4.7\times10^4$/ml	0.00008	0.0007
	Bromide	–	780 mg/l	0.72	79

[a]Average flow rate was 3.9 ml/min and specific discharge rate was 15 cm/day.
[b]Based on average injection concentration.
[c]Recovery calculated based on 22 l effluent volume for both experiments.

point-counted using a Nikon Optiphot microscope (1000 × magnification). Point-counting was performed on at least fifteen random fields for each filtered sample and serial dilutions were performed to reduce sample concentrations to levels necessary for optimum reproducibility ($\sim 10^6$ microspheres per slide; Harvey et al., 1989).

Bromide, in the form of a $CaBr_2$ solution (0.006 M in exp. #1, and 0.005 M in exp. #2) was used as a solute tracer in the experiments. The microspheres were added to the bromide solution, which displaced the $CaCl_2$ solution during injection. Bromide concentration in the effluent samples was measured using a pH/ISE analyzer equipped with a bromide electrode and double junction reference electrode.

3.3. Tracer experiments

In the first tracer experiment, four sizes of microspheres (0.05, 0.1, 0.5 and 1.0 μm diameter) were added to the tracer solution containing 0.006 M $CaBr_2$. In the second tracer experiment the sizes of microspheres were 0.5, 1.7 and 4.25 μm. For both experiments, flow rate was held constant at 3.9 ml/min during the tracer injection and subsequent flushing period. The average measured hydraulic gradient during the experiments was 0.08. During each experiment approximately 10.6 l of tracer solution ($CaBr_2$ plus microspheres) was pumped through the column, followed by flushing with at least 22 l of the $CaCl_2$ solution. The effluent was continuously sampled using a fraction collector and 15 ml polypropylene conical centrifuge tubes ($\sim$ 12 ml per sample).

3.4. Fracture and tracer distribution

The column was dismantled 105 days after the start of the tracer experiments and the distribution of fractures and microspheres were mapped under plain and ultraviolet light. Small 'microcore' samples of the fluorescent-stained soils were taken from the fracture surfaces, or the matrix between fractures, by scooping up approximately 5 mg of soil with an 18 gauge biopsy needle. Each soil sample was placed in a bottle with 10 ml of an eluent solution with a pH of 8 and then was placed in a sonic bath for 15 min to help remove the microspheres from the soil. After soaking for 24–48 h the soil solution was then filtered and the concentrations of each microsphere size (reported as number of microspheres per milligram of dry soil) were counted under an epi-fluorescent microscope.

4. Results of column experiments

4.1. Porosity and hydraulic conductivity

Eighteen soil samples collected from the field site were tested for porosity by determining the dry bulk density of each sample using the paraffin clod method (Blake and Hartge, 1986). The dry bulk density of the samples ranged from 1.34–1.74 g/cm^3, with an average of 1.56 g/cm^3. Porosity values ranged from 0.33–0.47 with an average of 0.42. The total pore volume of the saprolite column was 5.3 l. The average measured

hydraulic conductivity value for the sample before the tracer tests was 2.2×10^{-5} m/s. The average hydraulic conductivity values measured after the first and second tracer experiments were 2.3×10^{-5} m/s and 2.6×10^{-5} m/s, respectively, which showed that introduction of the colloidal tracers did not significantly change the hydraulic conductivity of the column.

4.2. Experimental breakthrough curves

The breakthrough curves (BTC) from both experiments indicate that there is an optimum size (approximately 0.5 μm) for transport of microspheres in this material. In both the injection and flushing portions of the experiments, relative concentrations of the 0.5 μm diameter microspheres were higher than measured for larger or smaller spheres. The highest recovery values were also measured for the 0.5 μm microspheres, which indicate they had the lowest rates of retention.

Breakthrough curves of the relative concentration (C/C_0) of microspheres and bromide versus cumulative injection volume for experiment #1 (Fig. 2a) showed that all four sizes of microspheres had rapid initial breakthrough followed by a period of constant or slowly decreasing concentrations. First arrival of the microspheres in the effluent occurred within 0.04 to 0.1 l of injection, indicating maximum travel velocities of 15 to 32 m/day. The first arrival of all the tracers occurred at much less than 1 PV (5.3 l) indicating that transport, at least initially, occurred mainly through fractures and macropores. First arrival of the bromide tracer occurred within 0.2 l, indicating a maximum travel velocity of 8.4 m/day. The microsphere concentrations reached a 'peak' value within 0.43 to 0.54 l of injection and then declined slightly to a 'plateau' value that was relatively constant after 1 to 4 l of injection. The bromide tracer also exhibited a rapid rise in concentration during the first 1 to 2 l of injection, but values did not reach a peak or plateau and continued to slowly increase for the entire 10.7 l duration of the tracer injection (Fig. 2b).

Injection tracer concentrations were measured periodically during the experiment and remained nearly constant (Table 1). The maximum C/C_0 obtained for each of the different microsphere tracers varied according to size, with the 0.5 μm diameter microspheres having the highest value (Table 1). The highest plateau C/C_0 was also observed for the 0.5 μm spheres. The bromide tracer reached a maximum C/C_0 of 0.81, which was up to $\sim$700 times higher than values observed for the microspheres.

During the flush portion of the breakthrough curves (Fig. 2b), C/C_0 values of all microsphere sizes initially dropped more rapidly than values for the bromide tracer. After 1–2 l of flushing the microsphere C/C_0 values declined at a slower rate, resulting in an extended low C/C_0 'tail'. The relative order of microsphere concentrations, in terms of particle size, were the same in the flush as in the tracer injection, with 0.5 μm diameter spheres having the highest C/C_0.

Breakthrough curves for microspheres and bromide for experiment #2 (Fig. 3a and b) showed that two of the three microsphere sizes (0.5 and 1.7 μm) had rapid initial breakthrough followed by a periods of slowly increasing, then steady C/C_0. The largest size microspheres (4.25 μm) appeared sporadically in effluent samples, but stayed below the detection limit throughout most of the experiment. First arrival of 0.5 and 1.7 μm

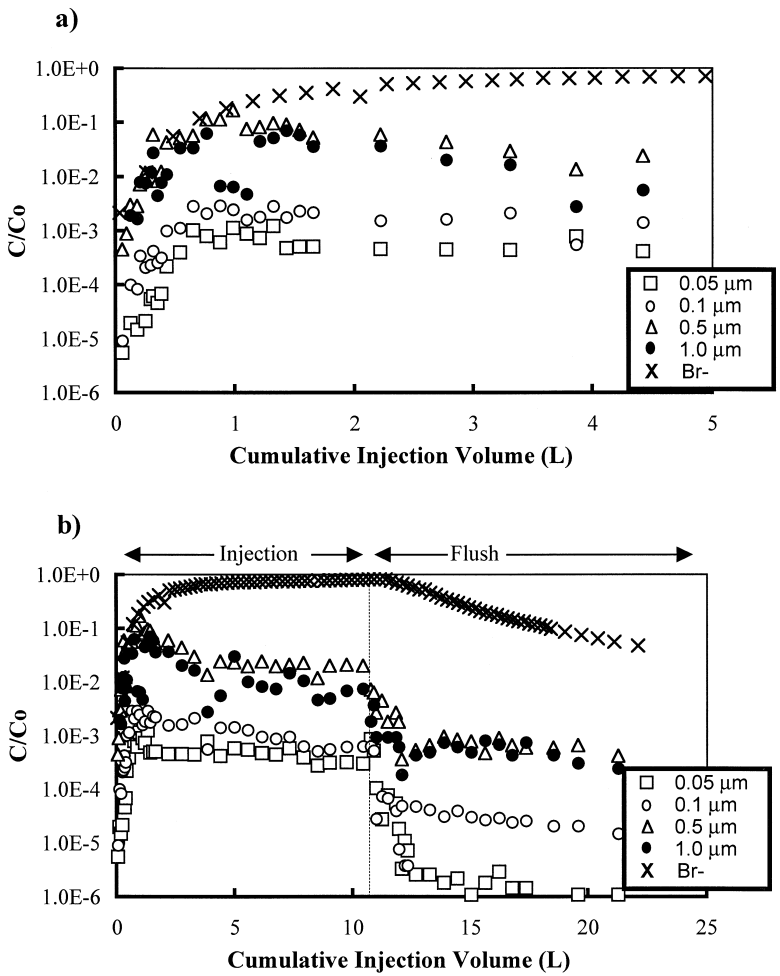

Fig. 2. Semi-logarithmic plot of (a) early time breakthrough curves for tracer experiment #1, and (b) complete breakthrough curves for experiment #1.

microspheres occurred within 0.05 l (0.009 PV) of the start of injection and first arrival of 4.25 µm diameter microspheres occurred within 0.53 l (0.1 PV). The first arrival times indicated maximum travel velocities ranging from 3.8 to 27 m/day. First arrival of bromide (relative to background concentration) occurred within 0.5 l of the start of injection, indicating a maximum travel velocity of 4.2 m/day.

The maximum C/C_0 observed during experiment #2 for each of the different microsphere tracers (Table 1) varied by size, with the 0.5 µm diameter microspheres having the highest value at 0.036, followed by the 1.7 µm size at 0.0057. The maximum C/C_0 reached by the 4.25 µm size was 8.0×10^{-5}. During the first 5 l of injection, C/C_0 values for the 0.5 µm diameter microspheres, which was the only size used in both experiments, were lower than observed in experiment #1. From 5–10 l of

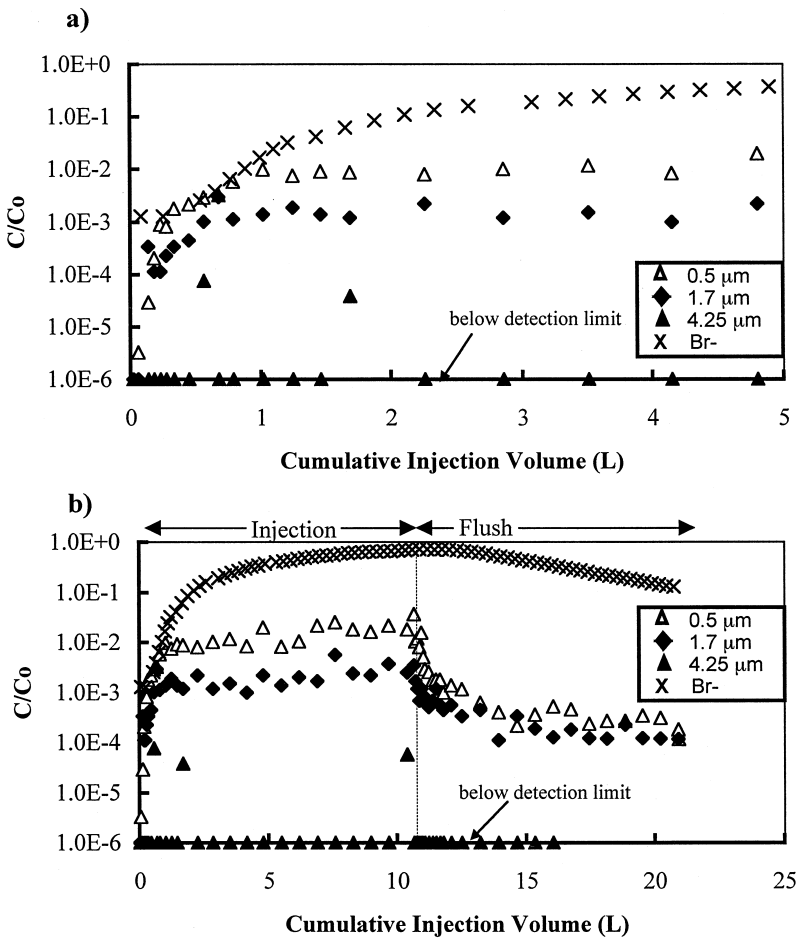

Fig. 3. Semi-logarithmic plot of (a) early time breakthrough curves for tracer experiment #2, and (b) complete breakthrough curves for experiment #2.

cumulative injection volume, the relative concentrations of the 0.5 μm size were approximately the same for both experiments. It is not clear what caused the difference in relative concentrations of the 0.5 μm diameter microspheres in experiments #1 and #2, but in both cases relative concentrations of the 0.5 μm size were higher than for any of the other microspheres. Relative bromide concentrations in experiment #2 were also slightly lower than in experiment #1 (maximum C/C_0 values of 0.81 and 0.72 for experiments #1 and #2, respectively) and again it is not clear what caused this difference.

During the flush portion of experiment #2 BTC (Fig. 3b), the C/C_0 of the 0.5 and 1.7 μm microspheres initially dropped more rapidly than values for bromide (the 4.25 μm microspheres were not detected during flush). After 1–2 l of flushing, microsphere C/C_0 declined more slowly, resulting in low C/C_0 tails, similar to those observed in

experiment #1. The relative order of microsphere C/C_0 during flush, in terms of particle size, remained the same as during injection, with the 0.5 μm diameter spheres having the highest value.

4.3. Mass balance

Mass balance calculations were performed by integrating the area under the breakthrough curves for each tracer. Results of the mass balances (Table 1) show a very low percentage of recovery for all microsphere sizes (0.0007 to 1.4%) compared to bromide (79 to 93%). The 0.5 μm microspheres exhibited the greatest recovery and hence the least retention. The relative order of microsphere recovery for the different sizes corresponds directly to the order of maximum C/C_0 observed in the effluent. The total volume of microspheres retained in the column was approximately 0.35 ml which was only 0.24% of the estimated fracture volume (150 ml), calculated based on the measured hydraulic conductivity and fracture spacing using the cubic law (Snow, 1969). This indicates that colloid retention during the experiments was unlikely to cause significant clogging of the fractures and was consistent with the measured values of hydraulic conductivity, which showed essentially no change during the experiments.

4.4. Fracture and microsphere distribution mapping

Inspection of the dissected saprolite column under ambient light showed three sets of fractures, the first occurring along bedding planes (BP), with the two other sets nearly orthogonal (O) to bedding. The bedding plane set had fracture spacings of 5–30 mm (mean of 9 mm), while the orthogonal fracture sets both had spacings of 20–30 mm (mean of 27 mm). The saprolite is weathered throughout to a mottled yellowish brown and reddish brown color. Black staining, likely due to oxidation of manganese, was observed on about 50% of the bedding plane fractures, and on $< 10\%$ of the orthogonal fractures.

Inspection of the column under an ultraviolet (UV) light source showed that the microspheres, which were visible as blue or yellow-green fluorescent staining, were present mainly on fracture surfaces, except within approximately 1 cm of the influent end of the column, where fluorescence was also visible in the matrix. Under UV light approximately 50% of the BP fractures exhibited blue or yellow-green fluorescent staining, mostly on fractures that did not have extensive black oxidation staining. This suggests that either the black-stained bedding plane fractures were ‘closed’ during the experiment, or that the microspheres did not readily attach to these surfaces. Nearly all of the O fractures had at least some fluorescent staining along their surfaces, indicating that they were active flow pathways during the tracer experiments.

The fluorescent staining visible under UV light tended to be most intense along fracture intersections, but also occurred as irregularly-shaped regions on fracture surfaces (Fig. 4). In some cases the fluorescent staining formed sharply defined dendritic patterns. Typically the fluorescent-stained area of a fracture was small (10 to 30%) relative to the surface area of the fracture. Intensity of fluorescent staining decreased

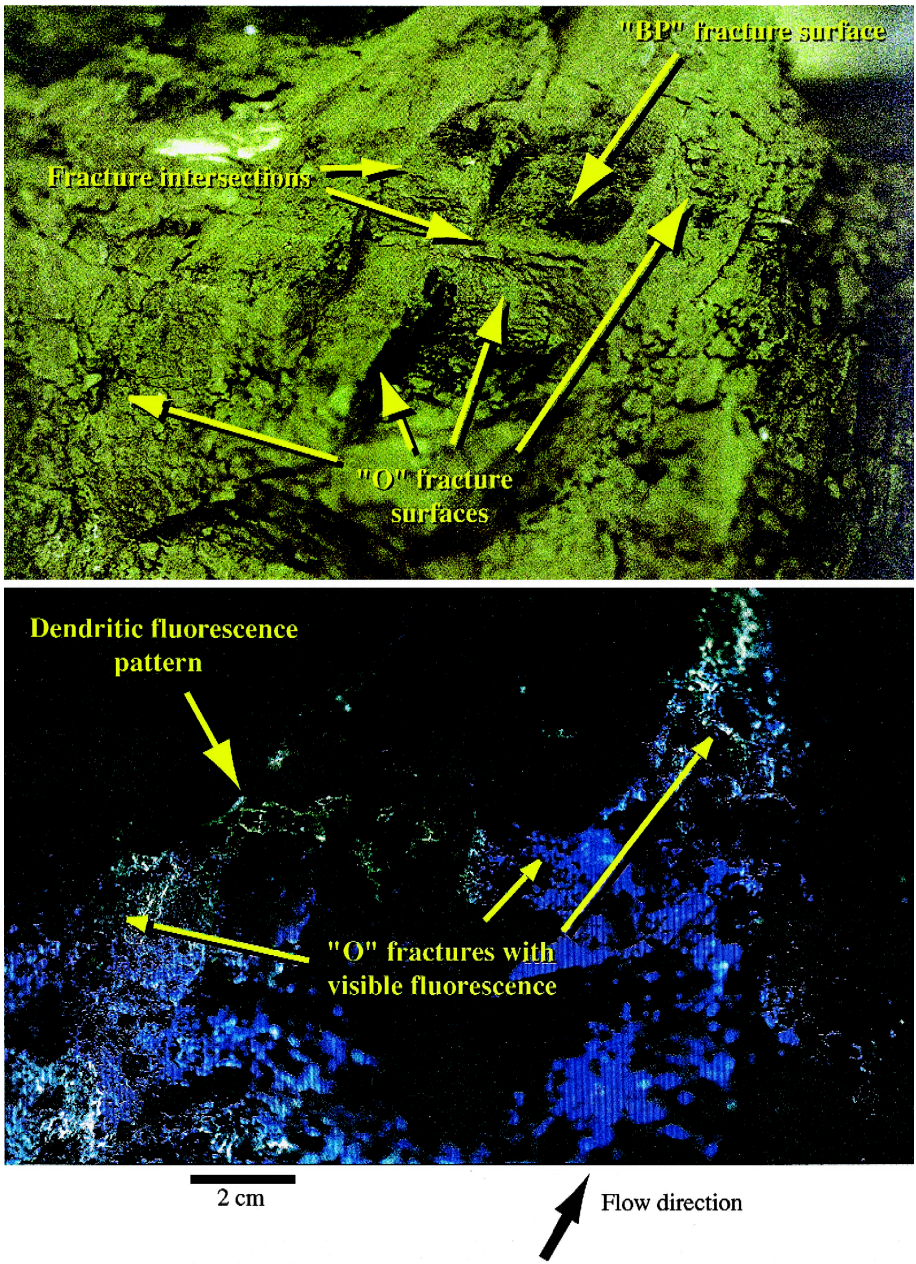

Fig. 4. Photographs showing fractures under ambient and UV light.

with distance from the inlet, although fluorescent stains were observed throughout the entire length of the column. The fluorescent staining varied from an intense blue to a

bright green; in some cases the color change was gradational and in other cases the change was abrupt. This is believed to be due to size-segregation of the microspheres between fractures of different aperture or between larger and smaller aperture regions, or 'channels', within the same fracture. Because only two colors were used for the six different sizes of microspheres, it was not possible to visibly distinguish between regions where the larger and smaller microspheres were retained.

Measurements of the concentration of microspheres determined from microcore samples taken along an extensive BP fracture are shown on Fig. 5. Concentrations of the

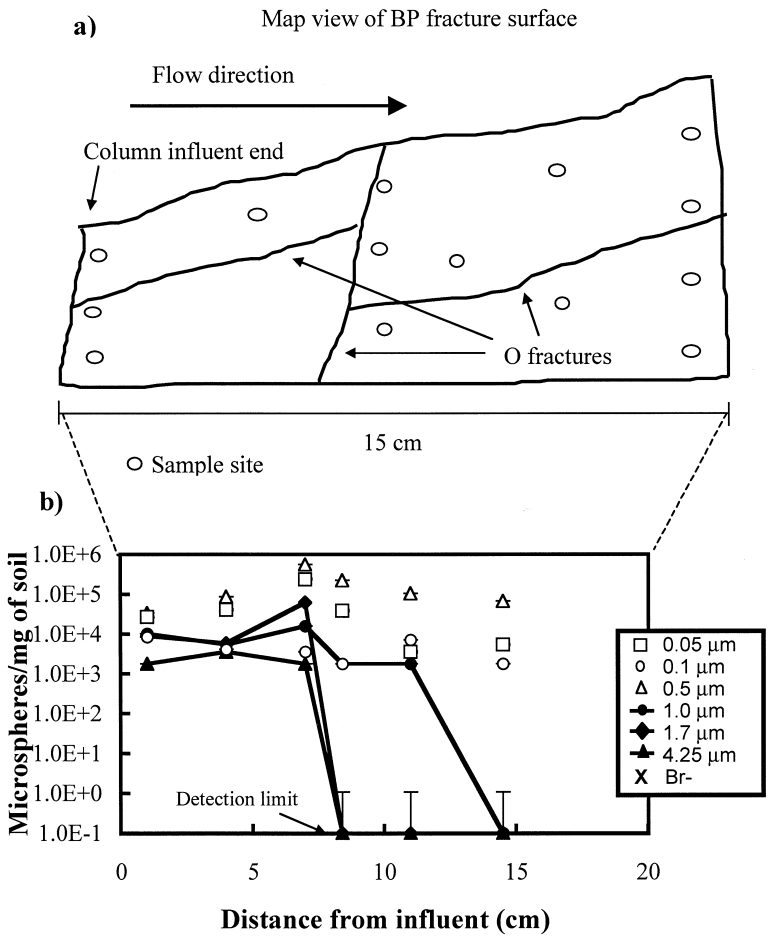

Error bars for most data points smaller than size of data icon.

Fig. 5. (a) Locations of samples taken from surface of a BP fracture, and (b) concentration of microspheres versus distance away from influent end of column along the same BP fracture surface (values plotted are average of all samples taken at each distance).

smaller size microspheres (0.05, 0.1, and 0.5 μm) remained consistently high with increasing distance from the influent end of the column, while concentrations of the larger sizes (1.0, 1.7, and 4.25 μm) decreased abruptly after a travel distance of 8–11 cm, likely due to straining or gravitational settling.

Measurements of microsphere concentrations along a fracture where there were dendritic 'channels' defined by fluorescence under UV light are shown on Fig. 6. The measurements show the highest microsphere concentrations occurred in the brightest channel, but peaks were also observed at sites where fluorescence was more diffuse. The profile shows that microsphere retention along a fracture surface can be highly variable.

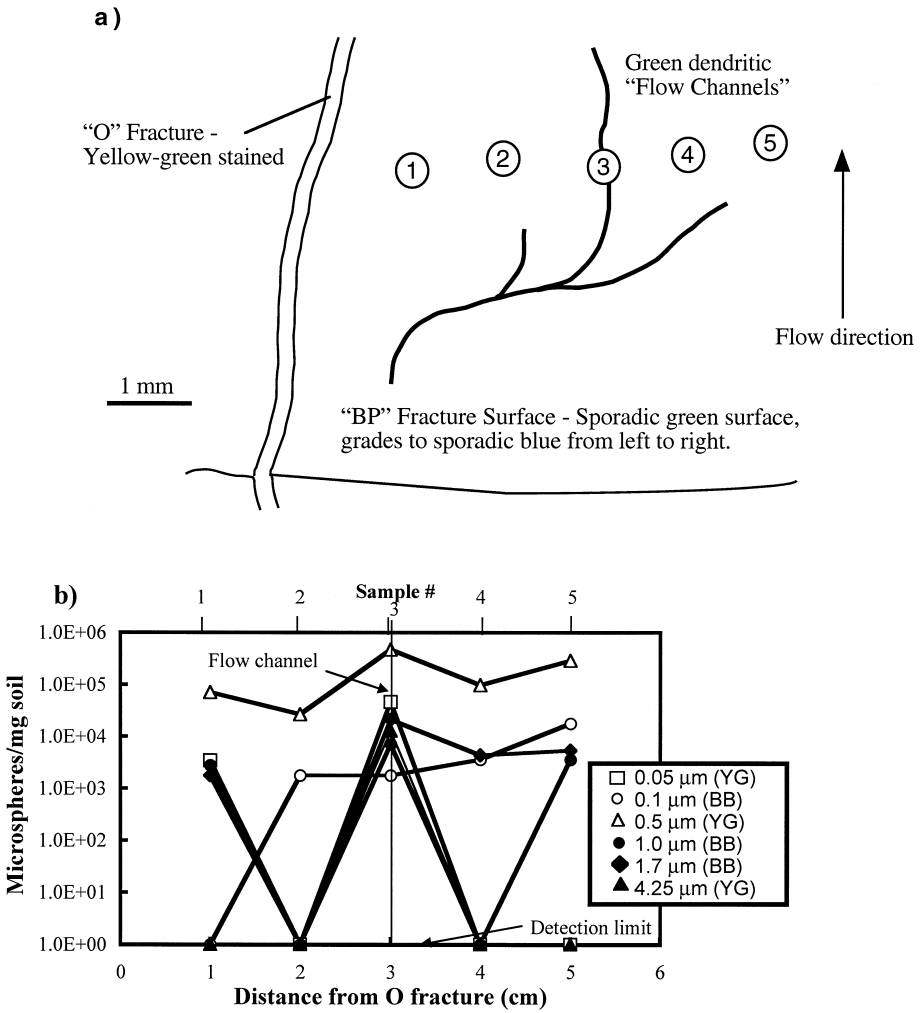

Fig. 6. (a) Diagram showing sampling sites, and (b) graph of concentration of versus distance from fracture intersection.

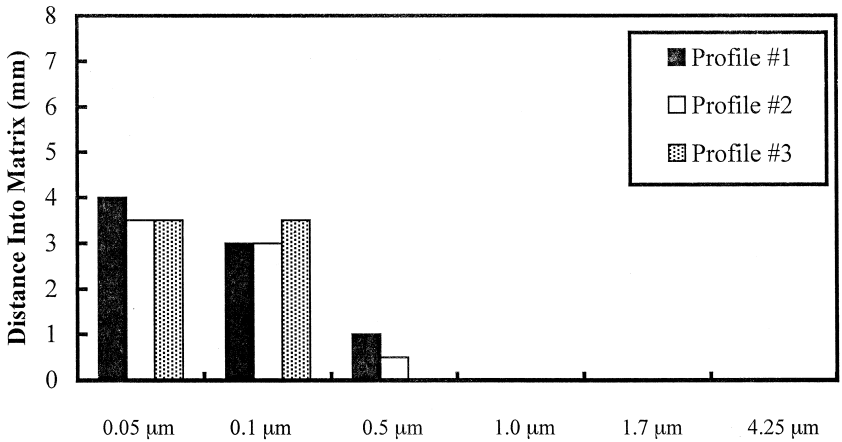

Fig. 7. Profiles of depth of penetration of microspheres into fine-grained matrix adjacent to fractures.

Microcore samples were also taken from the blocks of fine-grained matrix between fractures to determine if any of the microspheres had penetrated the matrix. These were taken several days after the column was dissected and the soil was dry. There were very few microspheres visible on the filter and those that were visible were usually within soil aggregates, so it was not possible to accurately measure concentration. However, for each size of microsphere it was possible to determine the maximum distance of migration away from the nearest fluorescent-stained fracture. This type of sampling was done for two BP fractures (Profiles 1 and 2) and an O fracture (Profile 3) as shown on Fig. 7. The smallest microspheres (0.05 and 0.1 μm) were found in the matrix up to 3–4 mm from the fracture surface, while sizes larger than 0.5 μm were not found in the matrix. The detection of microspheres in the matrix samples confirms that at least some of the smaller microspheres can enter the pores of the matrix.

5. Discussion of colloid transport and retention processes

5.1. Overview

The observed optimum colloid size (approximately 0.5 μm) for transport through the saprolite sample is consistent with predictions based on the conceptual models for colloid retention in fractured materials presented by Reimus (1995): namely greater loss of larger than optimum particles due to gravitational settling and straining in small aperture regions, combined with greater attachment of smaller than optimum particles because of higher diffusion rates within the fracture and hence more frequent collisions with fracture walls. The presence of the smallest microspheres (0.05 and 0.10 μm) in the matrix at distances of 3–4 mm from the nearest stained fracture also suggests that diffusion into the matrix or other regions of relatively immobile pore water can contribute to size-related segregation of particles. The relative importance of the

different retention mechanisms in the saprolite cannot be determined from simple inspection of the breakthrough curves and development of a numerical or analytical flow and transport model which explicitly includes these processes is beyond the scope of this study. However, some simple calculations described in the following sections were used to help assess the probable significance of different loss processes and to aid in the design of future experimental or modeling studies.

5.2. Fracture aperture and flow velocity

The 'average' fracture aperture, $2b$, for the column was calculated using an equation for two sets of vertical, constant aperture, parallel fractures, oriented orthogonal to one another (McKay et al., 1993a):

$$2b = \left[\frac{K_z 2B6\mu}{\rho_w g} \right]^{\frac{1}{3}} \tag{1}$$

where $2B$ is the fracture spacing, ρ_w is the fluid density of water, g is the gravitational constant, μ is the dynamic viscosity of water and K_z is the measured vertical hydraulic conductivity of the saprolite column. Eq. (1) is derived from the 'cubic law' (Snow, 1969), which is based on an analogy to flow between two smooth parallel plates. Because of the large difference between the pore sizes of the matrix and the much larger fractures, all flow was assumed to be in the fractures. The value of fracture spacing ($2B$) used in these calculations was 25 mm, which corresponds to the approximate spacing of fractures containing fluorescent staining from the microspheres.

The calculated hydraulic fracture aperture for the column was 71 μm, which was much larger than any of the microspheres used in this study. The largest microspheres (4.25 μm in diameter) were nearly immobile in the column but were still a factor of 16 smaller than the calculated aperture. This suggests that either straining did not play a major role in colloid retention during the experiments, or that cubic law aperture values, which integrate the effect of larger and smaller aperture regions, are not a reliable indicator of the likelihood of straining.

The flow velocity, v, in the fractures was also calculated from the cubic law based on the aperture and the measured hydraulic gradient, i, using (McKay et al., 1993a):

$$v = \frac{i(2b)^2 \rho_w g}{12\mu} \tag{2}$$

The calculated cubic law flow velocity of 29 m/day was approximately equal to the colloid transport velocities calculated based on first arrival of the microspheres in tracer experiments #1 (34 m/day) and #2 (30 m/day). This suggests that the cubic law can be useful for predicting advective colloid transport rates.

5.3. Settling rates

Gravity-driven settling rates for each microsphere size were calculated to determine if settling was likely to have had an impact on colloid losses during the tracer experiments.

In the column tracer experiments many of the fractures (especially the BP fractures) were nearly vertical, which would tend to reduce the importance of settling, but there were also some non-vertical fractures. As well, even in a vertical fracture there may be significant settling onto asperities on the rough walls of the fracture. The settling rates, or terminal velocities, v_t were calculated using an equation based on Stoke's law for settling of a dense sphere in a viscous fluid (Kane and Sternheim, 1988):

$$v_t = \frac{2R^2}{9\mu} g(\rho - \rho_w) \tag{3}$$

where ρ is the density of the particle and R is the radius of the particle.

The calculated settling rates ranged from 5.4×10^{-7} m/s for the 4.25 μm diameter microspheres, to 7.5×10^{-11} m/s for the 0.05 μm microspheres. For the calculated settling rates, the largest microsphere (4.25 μm) would settle 490 μm during the calculated 900 s residence time of the flowing water in the column, while the 1.0 and 1.7 μm microspheres would settle 27 and 78 μm, respectively. This would be sufficient time for many of the larger microspheres to settle out in an 'average' 71 μm aperture fracture, indicating that gravitational settling is likely an important process for the larger microspheres. For the smaller microspheres, settling distances during the 900 s residence time were much less (0.07 to 6.7 μm) and hence retention by settling was expected to be less.

5.4. Influence of diffusion

Diffusion of colloids from the fast flowing central region of the fractures to the fracture walls was simulated by using the calculated diffusion coefficient, determined from the Stokes–Einstein equation (Einstein and Furth, 1926), and a 1-dimensional solution to Fick's second law (Crank, 1956):

$$\frac{C}{C_0} = \operatorname{erfc} \frac{x}{2\sqrt{Dt}} \tag{4}$$

where C/C_0 is the relative concentration of microspheres at a distance, x, from a constant concentration source at an elapsed time, t. In this case we assumed a constant concentration of microspheres at the center of a fracture and then calculated the resulting concentration at the fracture wall, 35 μm away, after 900 s. The actual concentration profile within the fractures is unknown but this simplification is expected to provide an indication of the relative importance of diffusion on retention of the different sizes of microspheres. For the two smallest sizes of microspheres (0.05 and 0.1 μm) the relative concentration at the fracture walls would be high, 0.58 and 0.43, respectively. This could significantly increase the number of collisions with the fracture walls and increase attachment losses for these sizes. For the larger sizes calculated relative concentrations at the fracture wall were much lower (0.07 to < 0.001), hence there would be less attachment loss.

Quantifying diffusion of microspheres in or out of relatively immobile pore water in the matrix or in small aperture regions of the fractures is more difficult because the

distribution of flow within the fractured saprolite is not well understood. A simple calculation was carried out to determine whether diffusion into the matrix could have accounted for the penetration of the smaller microspheres (0.05 and 0.1 μm) a distance of up to 4 mm from the nearest fracture. The calculation assumes that there is a constant concentration of microspheres at the fracture wall and calculates the relative concentration at a distance of 4 mm in the matrix, for an elapsed time of 105 days, which is the time from the start of the tracer experiments to the dissection and drying out of the column. The diffusion coefficient values are the same as used for diffusion in the fracture, meaning that matrix tortuosity and attachment are neglected. The calculations indicate that concentrations of the smallest microspheres (0.05 and 0.1 μm) at a distance of 4 mm from the fracture wall could be as high as 0.52 and 0.36, respectively, of the concentration at the fracture wall. As expected, calculated relative concentrations of the larger microspheres were much smaller, ranging from 0.04 to < 0.001. Although these calculations suggest that diffusion could be responsible for the observed migration of the smallest microspheres into the matrix, it is expected that these losses were much smaller than losses due to diffusion-related collisions with the fracture walls. As well, other factors, such as advective transport into the matrix or transport related to drying of the column prior to collection of the microcores, may have contributed to migration into the matrix.

6. Conclusions

This study has shown that there is an optimum particle diameter, approximately 0.5 μm, for transport of carboxylate-coated latex microspheres in a sample of highly weathered and fractured shale. The behavior of the microsphere tracers is consistent with conceptual models typically used for colloid filtration theory in granular media, which predict greater losses of larger than optimum particles due to physical straining and settling, and losses of smaller than optimum particles due to faster diffusion and hence, greater likelihood of collision with and attachment to the fracture walls. Preliminary evaluation of the size-related loss processes with simple 1D analytical models suggest that for this experimental study, gravitational settling is an important process for retention of the larger than optimum particles, while diffusion-related collisions with the fracture walls is an important process for retention of the smaller than optimum particles.

Microsphere distribution mapping shows that the microspheres were transported mainly through the fractures, with about half of the visible fractures showing fluorescent staining from the microspheres. The greatest concentrations of microspheres tended to occur at fracture intersections and in ‘channels’ along fracture surfaces. Measurements of microsphere concentrations in microcore samples taken from the fracture surfaces clearly show that there is size segregation of the microspheres along the fracture surfaces and in the channels or intersections. Microcore samples taken from within the matrix adjacent to the fractures show that smaller particles can migrate, presumably by diffusion, distances of at least a few millimeters into the fine pore structure of the matrix, but it is expected that losses due to this mechanism were small.

The principal findings of this study, namely the existence of an optimum size for colloid transport in the sample of shale saprolite, and size-segregation of microspheres between different fractures or regions of fractures, are expected to be applicable to other fractured clay-rich materials, such as tills and lacustrine deposits. Further studies are needed to determine the importance of particle diameter relative to other factors influencing retention, such as flow velocity, solution pH and ionic strength.

Acknowledgements

The authors wish to thank Drs. J.F. McCarthy and G. Moline at Oak Ridge National Laboratory, and the reviewers, including Drs. R. Bales (Univ. Arizona) and P. Vilks (Whiteshell Laboratories, Canada). We are indebted to Dr. G. Sayler and the UT—Center for Environmental Biotechnology for providing laboratory facilities and equipment. This research was supported by funds from the Water Resources Research Center, the Waste Management Research and Education Institute and Oak Ridge National Laboratory through the US Dept. of Energy—Environmental Management Science Program. ORNL is managed by Lockheed Martin Energy Research for DOE under contract number DE-AC05-96OR22464.

References

Bales, R.C., Gerba, C.P., Grondin, G.H., Jensen, S.L., 1989. Bacteriophage transport in sand soil and fractured tuff. Applied and Environmental Microbiology 55 (8), 2061–2067.

Bales, R.C., Li, S., Maguire, K.M., Yahya, J.T., Gerba, C.P., 1993. MS-2 and Poliovirus transport in porous media: hydrophobic effects and chemical perturbations. Water Resources Research 29 (4), 957–963.

Bales, R.C., Li, S., Maguire, K.M., Yahya, M.T., Gerba, C.P., Harvey, R.W., 1995. Virus and bacteria transport in a sandy aquifer, Cape Cod, MA. Ground Water 33 (4), 653–661.

Blake, G.R., Hartge, K.H., 1986. In: Black et al. (Eds), Bulk density. In: Methods of Soil Analysis, Part 1. Physical and Mineralogical Methods—Agronomy Monograph no. 9, 2nd end., C.A., pp. 383–390.

Champ, D.R., Schroeter, J., 1988. Bacterial transport in fractured rock—a field-scale tracer test at the Chalk River Nuclear Laboratories. Water Sci. Technol. 20, 81–87.

Crank, J., 1956. The Mathematics of Diffusion. Oxford Univ. Press, Oxford.

Cropper, S.C., 1998. Experimental measurements of capillary pressure-saturation drainage of air and DNAPL in fractured shale saprolite. Masters Thesis, Dept. of Geol. Sci., University of Tennessee, Knoxville.

Cumbie, D.H., 1997. Laboratory scale investigations into the influence of particle diameter on colloid transport in highly weathered and fractured shale saprolite. Masters Thesis, Dept. of Geol. Sci., University of Tennessee, Knoxville.

Einstein, A., Furth, 1926. Investigations on the theory of the Brownian movement. Cowper, A.D., translation. Methuen, London.

Elimelech, M., O'Melia, C.R., 1990. Kinetics of deposition of colloidal particles in porous media. Environmental Science and Technology 24, 1528–1536.

Fontes, D.E., Mills, A.L., Hornberger, G.M., Herman, J.S., 1991. Physical and chemical factors influencing transport of microorganisms through porous media. Applied Environmental Microbiology 57, 2473–2481.

Harton, A.D., 1996. Influence of flow rate on transport of bacteriophage in a column of highly weathered and fractured shale. Master's Thesis. Dept. Of Geol. Sci., University of Tennessee, Knoxville.

Harvey, R.W., George, L.H., Smith, R.L., LeBlanc, D.R., 1989. Transport of microspheres and indigenous

bacteria through a sandy aquifer: results of natural-and forced-gradient tracer experiments. Environmental Science and Technology 23, 51–56.

Harvey, R.W., Kinner, N.E., MacDonald, D., Metge, D.W., Bunn, A., 1993. Role of physical heterogeneity in the interpretation of small-scale laboratory and field observations of bacteria, microbial-sized microsphere, and bromide transport through aquifer sediments. Water Resources Research 29 (8), 2713–2721.

Hatcher, R.D., Lemiszki, P.J., Dreier, R.B., Ketelle, R.H., Lee, R.R., Leitzke, D.A., McMaster, W.M., Foreman, J.L., Lee, S.Y., 1992. Status report on the geology of the Oak Ridge Reservation. Environmental Science Division Publication No. 3860, ORNL/TM-12074, Oak Ridge National Laboratory, Oak Ridge, TN.

Hinsby, K., McKay, L.D., Jorgensen, P., Lenczewski, M., Gerba, C.P., 1996. Fracture aperture measurements and migration of solutes, viruses, and immiscible creosote in a column of clay-rich till. Ground Water 34 (6), 1065–1075.

Jardine, P.M., Wilson, G.V., Luxmoore, R.J., 1988. Modeling the transport of inorganic ions through undisturbed soil columns from two contrasting water sheds. Soil Science Society of America Journal 52, 1252–1259.

Jardine, P.M., Jacobs, G.K., Wilson, G.V., 1993. Unsaturated transport processes in undisturbed heterogeneous porous media: I. Inorganic contaminants. Soil Science Society of America Journal 57, 945–953.

Kane, J.W., Sternheim, M. M., 1988. Viscous fluid flow. In: Physics, Wiley, New York, p. 355.

Kinoshita, T., Bales, R.C., Maguire, K.M., Gerba, C.P., 1993. Effect of pH on bacteriophage transport through sandy soils. Journal of Contaminant Hydrology 14, 55–70.

Kretzschmar, R., Robarge, W.P., Amoozegar, A., 1995. Influence of natural organic matter on colloid transport through saprolite. Water Resources Research 31 (3), 435–445.

McCaulou, D.R., Bales, R.C., Arnold, R.G., 1995. Effect of temperature controlled motility on transport of bacteria and microspheres through saturated sediment. Water Resources Research 31 (2), 271–280.

McDowell-Boyer, L.M., Hunt, J.R., Sitar, N., 1986. Particle transport through porous media. Water Resources Research 22, 1901–1921.

McKay, L.D., Cherry, J.A., Gillham, R.W., 1993a. Field experiments in a fractured clay till: 1. Hydraulic conductivity and fracture aperture. Water Resources Research 29 (4), 1149–1162.

McKay, L.D., Cherry, J.A., Gillham, R.W., 1993b. Field experiments in a fractured clay till: 2. Solute and colloid transport. Water Resources Research 29 (12), 3879–3890.

McKay, L.D., Sanford, W.E., Strong-Gunderson, J.M., De Enriquez, V., 1995. Microbial tracer experiments in a fractured weathered shale near Oak Ridge, Tennessee. Paper presented at Intl. Assoc. Hydrogeologists Congress, June 5–9, Edmonton, Alberta, Canada.

Meinders, J.M., Noordmans, J., Busscher, H.J., 1992. Simultaneous monitoring of the adsorption and desorption of colloidal particles during deposition in a parallel plate flow chamber. Journal of Colloidal and Interface Science 152 (1), 265–280.

Polysciences, 1995. Product Catalog. Warrington, PA.

Reimus, P.W., 1995. The Use Synthetic Colloids in Tracer Transport Experiments in Saturated Rock Fractures. LA-13004-T, Los Alamos National Laboratory, Los Alamos, NM.

Smith, M.S., Thomas, G.W., White, R.E., Ritonga, D., 1985. Transport of *Escherichia coli* through intact and disturbed soil columns. Journal of Environmental Quality 14 (1), 87–91.

Snow, D.T., 1969. Anisotropic permeability of fractured media. Water Resources Research 5, 1273–1289.

Solomon, D., Moore, G.K., Toran, L.E., Dreier, R.B., McMaster, R.B., 1992. Status report: a hydrologic framework for the Oak Ridge Reservation. ORNL/TM-12026. Oak Ridge National Laboratory, Oak Ridge, TN.

Tan, Y., Gannon, J.T., Baveye, P., Alexander, M., 1994. Transport of bacteria in an aquifer sand: experiments and model simulations. Water Resources Research 30 (12), 3243–3252.

Toran, L.E., Palumbo, A.V., 1992. Transport of bacteria-sized particles through fractured and unfractured laboratory sand columns. Journal of Contaminant Hydrology 9, 289–303.

Vilks, P., Bachinski, D.B., 1996. Colloid and suspended particle migration experiments in a granite fracture. Journal of Contaminant Hydrology 21, 269–279.

Vilks, P., Frost, L.H., Bachinski, D.B., 1997. Field scale colloid migration experiments in a granite fracture. Journal of Contaminant Hydrology 26, 203–214.

Wang, D., Gerba, C.P., Lance, J.C., 1981. Effect of soil permeability on virus removal through soil columns. Applied and Environmental Microbiology 42 (1), 83–88.

Wilson, G.V., Jardine, P.M., O'Dell, J.D., Collineau, M., 1992. Field-scale transport from a buried line source in variably saturated soil. Journal of Hydrology 145, 83–109.

Wollum, A.G., Cassel, D.K., 1978. Transport of microorganisms in sand columns. Soil Science Society of America Journal 42, 72–76.

Yao, K.M., Habibian, M.T., O'Melia, C.R., 1971. Water and waste water filtration: concepts and applications. Environmental Science and Technology 5 (11), 1105–1112.